Form Approved
OMB No. 0704-0188

REPORT DOCUMENTATION PAGE

1. REPORT DATE *(DD-MM-YY)*	2. REPORT TYPE	3. DATES COVERED *(From - To)*
13-09-2016	Conference Proceedings	July 2013 - June 2016

4. TITLE AND SUBTITLE
Measuring Pulse Rate Variability using Long-Range, Non-Contact Imaging Photoplethysmography

5a. CONTRACT NUMBER

5b. GRANT NUMBER

5c. PROGRAM ELEMENT NUMBER

6. AUTHOR(S)
Ethan B. Blackford*, Alyssa M. Piasecki#, Justin R. Estepp°

5d. PROJECT NUMBER

5e. TASK NUMBER

5f. WORK UNIT NUMBER
H0AE (2311RC11)

7. PERFORMING ORGANIZATION NAME(S) AND ADDRESS(ES)

*Ball Aerospace and Technologies Corp.
2875 Presidential Dr.
Fairborn, OH, 45324

#Oakridge Institute for Science and Ed.
48110 Shaw Road, Unit 5.
Patuxent River, MD, 20670-1906

8. PERFORMING ORGANIZATION REPORT NUMBER

9. SPONSORING/MONITORING AGENCY NAME(S) AND ADDRESS(ES)
°Air Force Materiel Command
Air Force Research Laboratory
711th Human Performance Wing
Airman Systems Directorate
°Warfighter Interface Division
Applied Neuroscience Branch
Wright-Patterson Air Force Base, OH 45433

10. SPONSORING/MONITORING AGENCY ACRONYM(S)
711 HPW/RHCPA

11. SPONSORING/MONITORING AGENCY REPORT NUMBER(S)

12. DISTRIBUTION / AVAILABILITY STATEMENT
DISTRIBUTION STATEMENT A: Approved for public release; distribution unlimited.

13. SUPPLEMENTARY NOTES
88ABW Cleared 08/10/2016; 88ABW-2016-3957. Report contains color.

14. ABSTRACT
Camera-based measurement of the blood volume pulse via non-contact, imaging photoplethysmography is a very popular approach for measuring pulse rate using a remote imaging sensor. Comparatively less attention has been paid to the usefulness of the method for measuring features of pulse rate variability, and even less focus has been put on the accuracy of any cardiac activity feature that can be achieved at long imager-to-subject distances. In this study, video was recorded from 19 participants, while at rest, at a distance of 25 meters from the imaging sensor. A digital camera was used to record video while cardiovascular measures of both electrical and optical physiological ground truth were recorded. Pulse rate data obtained from the imager using a common blind source separation and periodogram approach were compared to physiological ground truth signals. The quality of the recovered blood volume pulse morphology was sufficient to calculate time-domain measures of pulse rate using inter-pulse interval (IPI) time series. Following this, several features of pulse rate variability were calculated from the IPI time series and compared to those calculated from the corresponding physiological ground truth signals. Use of the time-domain data as compared to the periodogram approach to measure pulse rate reduced the error in the estimate from 1.6 to 0.2 beats per minute. Correlation analysis (r^2) between the camera-based measures of pulse rate variability and ECG-derived heart rate variability ranged from 0.779 to 0.973; these results are of comparable outcome to those obtained at imager-to-subject distances of no more than 3 meters. This study demonstrates that pulse rates of less than one beat-per-minute error can be obtained when the recovered blood volume pulse morphology is of adequate quality to resolve systolic onsets for individual cardiac cycles. Further, this approach can yield data of very promising quality for estimating measures of pulse rate variability.

15. SUBJECT TERMS
Photoplethysmography, non-contact imaging photoplethysmography, long-range imaging, pulse rate, pulse rate variability, heart rate, electrocardiography, blind source separation, independent component analysis

16. SECURITY CLASSIFICATION OF:			17. LIMITATION OF ABSTRACT:	18. NUMBER OF PAGES	19a. NAME OF RESPONSIBLE PERSON
a. REPORT	b. ABSTRACT	c. THIS PAGE			Justin Estepp
Unclassified	Unclassified	Unclassified	SAR	8	19b. TELEPHONE NUMBER

Measuring Pulse Rate Variability using Long-Range, Non-Contact Imaging Photoplethysmography

Ethan B. Blackford, *Member, IEEE,* Alyssa M. Piasecki, and Justin R. Estepp, *Member, IEEE*

Abstract*— Camera-based measurement of the blood volume pulse via non-contact, imaging photoplethysmography is a very popular approach for measuring pulse rate using a remote imaging sensor. Comparatively less attention has been paid to the usefulness of the method for measuring features of pulse rate variability, and even less focus has been put on the accuracy of any cardiac activity feature that can be achieved at long imager-to-subject distances. In this study, video was recorded from 19 participants, while at rest, at a distance of 25 meters from the imaging sensor. A digital camera was used to record video while cardiovascular measures of both electrical and optical physiological ground truth were recorded. Pulse rate data obtained from the imager using a common blind source separation and periodogram approach were compared to physiological ground truth signals. The quality of the recovered blood volume pulse morphology was sufficient to calculate time-domain measures of pulse rate using inter-pulse interval (IPI) time series. Following this, several features of pulse rate variability were calculated from the IPI time series and compared to those calculated from the corresponding physiological ground truth signals. Use of the time-domain data as compared to the periodogram approach to measure pulse rate reduced the error in the estimate from 1.6 to 0.2 beats per minute. Correlation analysis (r^2) between the camera-based measures of pulse rate variability and ECG-derived heart rate variability ranged from 0.779 to 0.973; these results are of comparable outcome to those obtained at imager-to-subject distances of no more than 3 meters. This study demonstrates that pulse rates of less than one beat-per-minute error can be obtained when the recovered blood volume pulse morphology is of adequate quality to resolve systolic onsets for individual cardiac cycles. Further, this approach can yield data of very promising quality for estimating measures of pulse rate variability.

I. Introduction

Photoplethysmography (PPG), first pioneered in the 1930's, is a low cost, noninvasive method of detecting changes in blood volume using variations in transmitted or reflected light. In either case, changes in light absorption caused by the blood volume pulse (BVP) wave are measured using a photodetector. A more recently developed technique, imaging photoplethysmography (iPPG), uses an image sensor to measure the same phenomenon and can provide both spatial and temporal information about the BVP wave. iPPG may present particular advantages over traditional, contact PPG for incorporation into telemedicine applications or for patients with skin sensitivities (e.g. burn patients or neonates [1]-[3]). Unlike the single photodetectors employed in traditional PPG, iPPG also has the ability to take measurements over large areas of skin for increased signal-to-noise ratios, measuring pulse transit time [4], mapping skin perfusion [5], [6], wound healing [7], or blood oxygen saturation [8]. [9]. Several topical reviews have provided insight into the current state of the art, challenges, and areas for future research in the domain of iPPG [10]-[16]. In both contact and noncontact methods, the varying light intensities are processed and used to represent changes in vascular blood volume. Onset of the systolic phase of the cardiac cycle in the arterial system can be observed in the BVP and can be used to extract important cardiovascular measures such as pulse rate (PR), pulse rate variability (PRV), and respiration rate. Other measures such as peripheral blood oxygen saturation (SpO_2) and blood pressure may be achievable via iPPG, as well.

PRV, in particular, contains valuable information about the autonomic nervous system and sympathetic/ parasympathetic activation which are indicative of cardiovascular health and stress states. While heart rate variability has traditionally been measured using electrocardiography (ECG), several studies have shown that PRV extracted from PPG can often be used as a surrogate for heart rate variability (HRV), especially under resting conditions [17], [18]. In order to measure pulse rate variability from an acquired PPG waveform, cardiac intervals must be measured from individually identified BVP waves. The accurate identification of the QRS complex in ECG is relatively straightforward as compared to the reliable identification of systolic onset in the PPG wave. In any case, consistent identification of individual cardiac cycle onsets, with high temporal resolution, is of utmost importance for the accurate measurement of cardiac variability.

Various time- and frequency-domain measures of HRV are common with standards for their measurement established by a joint international taskforce [19]. Commonly used time-domain indices include standard deviation of successive normal to normal (NN) cardiac intervals (SDNN) and the square root of the mean squared differences of successive NN intervals (RMSSD). SDNN reflects the overall variability in a given segment while RMSSD estimates short-term components of HRV. Frequency-domain indices include metrics such as low-frequency (LF)/ Traube-Hering-Mayer (THM) variability in

*With appreciation, we acknowledge that this work is supported by the Air Force Office of Scientific Research (AFOSR) under Air Force Research Laboratory Task# 14RH07COR, 'Non-Contact Cardiovascular Sensing and Assessment'.

E. B. Blackford is with Ball Aerospace & Technologies Corp., Fairborn, OH 45324-6269 USA (phone: +1-937-938-3635; e-mail: Ethan.Blackford.ctr@us.af.mil).

A. M. Piasecki is with the Oak Ridge Institute for Science and Education, Wright-Patterson AFB, OH 45433-7951 USA (email: Alyssa.Piasecki.ctr@us.af.mil).

J. R. Estepp is with the 711th Human Performance Wing, Air Force Research Laboratory, Wright-Patterson AFB, OH 45433-7951 USA (phone: +1-937-938-3602; e-mail: Justin.Estepp@us.af.mil).

the 0.04 to 0.15 Hz range and high-frequency (HF)/ respiratory sinus arrhythmia (RSA) variability in the 0.15 to 0.4 Hz range [20]. HF primarily denotes effects of respiration and parasympathetic/ vagal input to the cardiac system; alternatively, LF is more challenging to interpret but is known to contain information about sympathetic input to the cardiac system. The potential to evaluate these measures in a non-contact and unobtrusive manner is a great advantage for iPPG based methods.

Previously, we demonstrated successful measurement of windowed pulse rate estimates using long-range imaging photoplethysmography for stationary subjects and imager-to-subject distances of 25, 50, and 100 meters. Increased error in the pulse rate estimates was seen at distances of 50 and 100 meters and was likely due to decreased reflected light availability at the image sensor with longer focal-lengths and smaller regions of interest in the image. Additionally, the introduction of systematic error resulting from measurements of PR using power spectral analysis of the iPPG waveform was noted [21]. Herein we expand on the analysis of that dataset and demonstrate the use of long-range imaging photoplethysmography at a distance of 25 meters for the measurement of one-minute windowed estimates of pulse rate (using individual cardiac cycle identification) as well as pulse rate variability measured over five-minute windows using SDNN, LF, and HF. Gold-standard comparisons were derived from simultaneous measurements of contact ECG and fingertip reflectance PPG. The iPPG signals measured at 50 and 100 meters were deemed to be too noisy to analyze for identification of individual cardiac intervals. While several previous studies have investigated the estimation of HRV using traditional PPG [17], [18], [24]-[29] or iPPG at relatively short distances ranging from several centimeters to 3 meters [30]-[35], this is, to our knowledge, the first demonstration using long-range iPPG to measure pulse rate variability.

II. Methods

A. Equipment Setup

Video imagery used in this study came from a subset of data previously collected by the authors [21] and was recorded using high-quality, mirrorless digital cameras (Panasonic Lumix DMC-GH4, Panasonic, Kadoma, Osaka, Japan) equipped with fully-manual, super-telephoto lenses (650Z-B, Rokinon, New York, NY, USA). The imager was mounted to a tripod 1.2 meters above floor level. From the original dataset, only the recordings with an imager-to-subject distance of 25 meters were used for this study.

The imager was positioned to center the participant horizontally in the image with their entire head and as much of their upper torso in the frame as possible. To achieve this, camera and lens parameters were: 650mm focal length, shutter speed of 1/30s, 400 ISO, 3200K white balance, a resolution of 1920x1080 pixels, and a frame rate of 29.97 fps. Videos were recorded with all-intra frame, H.264 compression at a maximum bit rate of 200 Mbps to a .MP4 file on an internal SD card (64GB Extreme PRO SDXC UHS-II, SanDisk, Milpitas, California, USA). Fig. 1 shows the experimental setup.

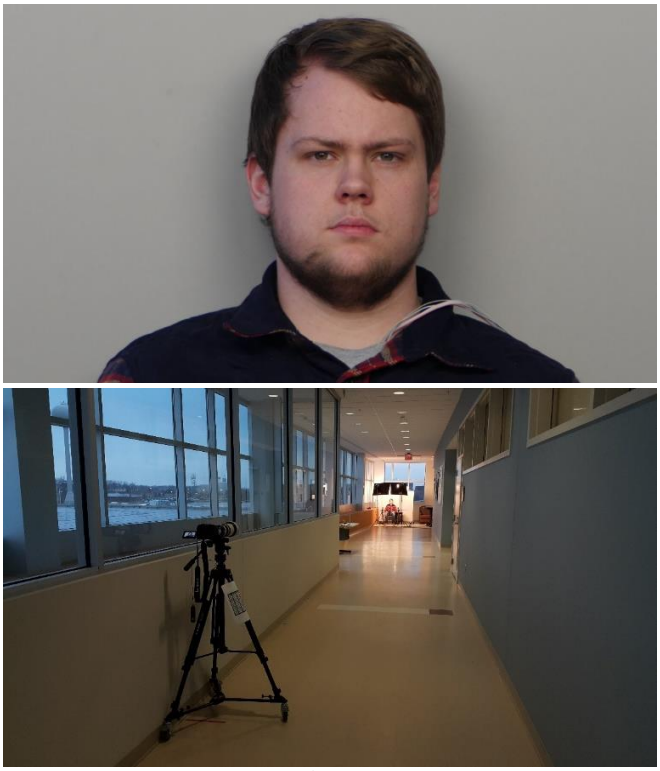

Figure 1. Characteristic images of the experimental setup. The top image image was captured using a 650mm super-telephoto lens and is characteristic of the frames analyzed in this study. The bottom image shows the imager setup at a distance 25m from the participant.

The experiment took place within a long, interior corridor of an office building with normal, ambient fluorescent lighting and a small amount of exterior light entering through windows on one side of the corridor. Two 1000W, 3200K, quartz-halogen light sources (QL-1000, Savage Equipment Products, Chandler, AZ, USA) mounted inside soft box diffusers were used as the illumination source. Each light source was placed 2m in front and 0.6m to either side of the subject, 2m above the ground, and directed toward the subject's face. The average experimental lighting conditions measured 970 lux using a Litemaster Pro L-478DF (Sekonic, North White Plains, New York, United States). A solid gray backdrop was placed behind the subject in order to reduce any signal noise from the image background.

Traditional, contact PPG ground-truth signals, along with synchronous recording of ECG, respiration, galvanic skin response (GSR), and a push-button trigger, were obtained using an ActiveTwo electrophysiological data acquisition system (BioSemi B.V., Amsterdam, The Netherlands) in which a single, continuous file was recorded to a workstation-class laptop running the acquisition software (ActiView, BioSemi B.V., Amsterdam, The Netherlands). Fingertip reflectance PPG was measured on the ring finger of the non-dominant hand from a fingertip reflectance sensor (MLT1020FC IR Plethysmograph Finger Clip, ADIntruments Inc., Colorado Springs, Colorado, USA) and ECG was measured from a bipolar pair of active electrodes positioned on the left clavicle and upper sternum. Respiratory effort, galvanic skin response (GSR), and video from three GoPro cameras positioned along a semi-circle in front of the subject were also recorded for each trial but not included in

this analysis and, therefore, not described in further detail here.

B. Subjects

A total of twenty-three participants (11 male, age range of 19-47 years old, mean age of 25.8 years) participated in this study after providing voluntary consent. One participant was excluded from the analysis due to a self-identified cardiac abnormality; in addition, three more participants were excluded due to low quality iPPG waveforms obtained during experimentation. Fig. 2 provides an example of the differentiation between low- and high-quality data for the exclusion process. This resulted in a total of nineteen participants available for analysis.

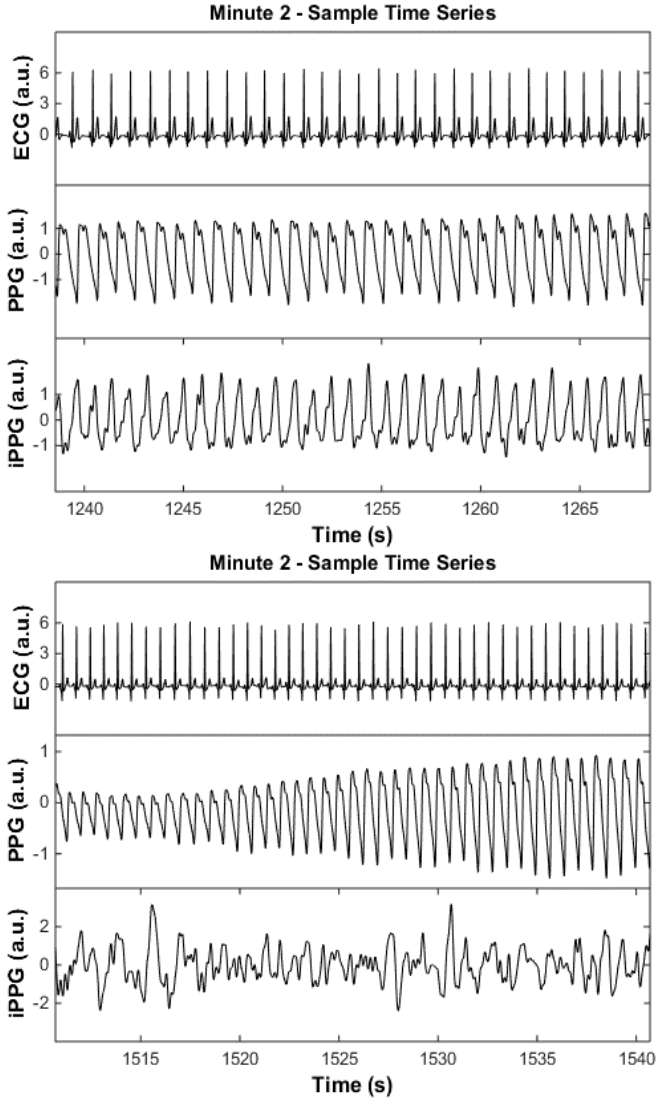

Figure 2. Comparison of high- and low-quality data for exclusion purposes. The top chart depicts high-quality data in which the iPPG waveform closely correlates with ground-truth ECG and PPG signals. The bottom chart depicts low-quality data excluded from analysis due to low correlation between waveforms. Note: As displayed, systolic onset in the PPG time series is represented as a valley while it is a peak in the iPPG time series.

The experimental protocol was reviewed and approved by the Air Force Research Laboratory Institutional Review Board and performed in accordance with all relevant institutional and national guidelines and regulations. All prospective participants received a study briefing and completed comprehensive written informed consent prior to their voluntary participation. Participants were compensated for their time unless otherwise employed by the Department of Defense and in duty status at the time of their participation. Skin tone, hairstyle, facial hair, clothing, glasses, piercings, and use of skin or beauty products were recorded but not otherwise used for analysis or screening purposes.

C. Experimental Design

Four trials were performed for each subject with each trial lasting approximately five minutes and twenty seconds. Both the first and last ten-second buffer segments were excluded from the analysis. Subjects were asked to look straight ahead and remain as still as possible during each trial. Of the full trial set [21], a single, randomly-selected trial recorded at a distance of 25 meters, per participant, was used for this analysis.

D. Ground Truth – ECG and PPG Signals

Raw ground truth ECG and PPG signals were processed into cardiac interval time series and subsequently windowed heart and pulse rates using custom software written in MATLAB 2011b (The Mathworks Inc., Natick, Massachusetts, USA). Individual trials within the video file were separated using the push-button trigger from the ActiView software and synchronized with the raw ground truth signals, sampled at 16 kHz. The time-aligned ECG and PPG signals were downsampled to 1200 Hz and filtered with a zero-phase, elliptical, bandpass filter with a pass band of 0.3-90 Hz and 0.3-16 Hz, respectively. The downsampled, bandpass-filtered signals were then normalized to zero-mean and unit-variance.

An automated R-wave detection algorithm [36], [37] was used to extract individual cardiac cycle times from the pre-processed ECG data and, similarly, an automated peak-finding algorithm with adaptive thresholding [38] was used to detect the fiducial point of the preprocessed PPG time series corresponding to the beginning of systole. All results from the automated algorithms were independently reviewed and hand-corrected by a subject-matter expert (SME) in order to identify any undetected or incorrectly identified points. Using the identified points corresponding to systolic onset, a cardiac interval time series was constructed consisting of inter-beat interval (IBI) and inter-pulse interval (IPI) time series for the ECG and PPG, respectively (generically, IXI time series). The IXI time series were segmented into 5, non-overlapping, 1-minute windows, and mean PR (from PPG) and HR (from ECG) for each window were calculated in beats per minute (bpm).

The periodogram method with a Hamming window was used to estimate mean pulse rates for each 1-minute window of the contact PPG segment, thus serving as an additional ground truth measure for pulse rate. This additional measure allows for comparison of time- (IPI) and frequency-domain (PSD) methods for estimating the PPG-based pulse rate. The pulse frequency was chosen as the frequency, f_{max}, with the highest power density occurring in the range from 0.8-2 Hz (approximating 48-120 bpm). This frequency was then converted to beats per minute ($60*f_{max}$).

E. Long Range iPPG – Image Series Data

A custom MATLAB analysis package was used to process the video file for each trial. The video was segmented into 5, non-overlapping, 1-minute segments. All RGB pixels were averaged over the entire frame, for each frame in a segment in order to produce the mean RGB time series. Each time series was normalized (within-segment) to zero-mean and unit-variance and bandpass filtered with a zero-phase, elliptical, bandpass filter from 0.3-11 Hz. Independent component analysis (ICA) was then used to decompose the normalized, bandpass-filtered, color-channel signals into independent RGB components. Following ICA, all independent components were bandpass filtered with a zero-phase, elliptical, bandpass filter between 0.3-6 Hz and upsampled to 1,200 Hz using cubic spline interpolation.

An estimate of signal-to-noise ratio (SNR) in the frequency range of the iPPG component signal was used to automatically choose the ICA component most likely to contain BVP information. This SNR estimate was calculated using the periodogram method with a Hamming window to locate the frequency with maximum power density within the range of 0.8-2 Hz. The band power for the dominant frequency was calculated over a range of ±0.123 Hz and transformed to relative power by dividing it by the component signal power falling outside the peak frequency range but within 0.8-2 Hz. The independent component with the highest relative power was chosen as the pulse rate component. As was performed for fingertip PPG, the frequency with the highest power density in the range of 0.8-2 Hz was chosen to represent pulse rate and converted to beats per minute ($60*f_{max}$).

F. Heart and Pulse Rate Estimate Comparison

The absolute value difference between pulse rate estimation methods was calculated to examine the accuracy of each method as compared to fingertip PPG with individual BVP identification. Fingertip PPG was chosen as the reference due to its known correlation with ECG at rest and better physiological correspondence with iPPG, since they both rely on the same underlying physiological phenomenon. For each of 5 corresponding, non-overlapping, 1-minute windows: (a) heart rate determined by the IBI time series from ECG, (b) pulse rate determined by periodogram of the fingertip PPG time series, (c) pulse rate by periodogram of the long-range iPPG time series, and (d) pulse rate determined by the IPI time series from long-range iPPG were subtracted from the pulse rate determined by the IPI series of fingertip PPG. Group mean absolute difference measures were bootstrapped 1000x via random selection of one of the 5, non-overlapping, 1-minute windows from each participant. The 95% confidence intervals on the bootstrapped means (1000 iterations) were calculated as an indicator of the range of the mean absolute error distribution for each participant.

G. Heart and Pulse Rate Variability Measures

To calculate pulse- and heart rate variability, the corresponding SME-corrected IPI and IBI time series derived from long-range iPPG and gold-standard ECG, respectively, were input to the CardioBatch software package [39]. CardioBatch was used to calculate frequency-domain HRV measures: LF/THM variability (0.06-0.10 Hz) and HF/RSA variability (0.12-0.40 Hz) and the time-domain, overall variability measure SDNN [40], [41]. To investigate the accuracy of PRV measurements derived from long-range iPPG as compared to gold-standard, ECG-derived HRV, side-by-side correlation and Bland-Altman plots [42], [43] were created for each measure of HRV: LF/THM, HF/RSA, and SDNN.

III. Results

A. Time Series Data

Above, in Fig. 2, a characteristic example of the high-quality, non-contact iPPG waveforms recovered for 19 of 22 participants at imager-to-subject distances of 25 meters is displayed. Individual BVP waves can be readily identified in the iPPG waveform and the timing of the pulse waves corresponds well with both the electrical cardiac activity observed in the ECG waveform and optical, contact measurement of the BVP waveform measured at tip of the ring finger.

B. Heart Rate and Pulse Rate

Corresponding one-minute windows were used to evaluate the accuracy of heart rate and pulse rate measurements as described in the previous section. Four pairings of windowed cardiac rate measurements were compared on basis of absolute difference. Each measurement method, listed below, was compared to fingertip PPG with individual BVP wave identification:

(a) Contact ECG with individual cardiac cycle identification (PPG_{IPI} – ECG_{IBI}). This pairing represents a best-case baseline comparison between measurements of cardiac rate recorded from participants at rest.
(b) Contact PPG using the dominant frequency in the windowed periodogram (PPG_{IPI} – PPG_{PSD}). This comparison is an estimate of the anticipated error in pulse rate measurement due to the PSD-derived method.
(c) Long-range iPPG using the dominant frequency in the windowed periodogram (PPG_{IPI} – $iPPG_{PSD}$). This comparison shows the accuracy of our previously published method for the detection of pulse rate using long-range iPPG and is subject to the error inherent in the periodogram method.
(d) Long-range iPPG with individual cardiac cycle identification (PPG_{IPI} – $iPPG_{IPI}$). This comparison shows the accuracy of pulse rates derived from long-range iPPG using IPI time series of individually identified systolic onsets in the BVP.

These group, mean absolute difference measurements were bootstrapped 1000x via random selection of one of the 5, non-overlapping, 1-minute windows from each participant and are displayed in the boxplots shown in Fig. 3.

C. Heart Rate Variability and Pulse Rate Variability

To investigate the accuracy of PRV measurements derived from long-range iPPG as compared to gold-standard, ECG-derived HRV, side-by-side correlation and Bland-Altman plots are displayed in Fig. 4 for each measure of HRV: LF/THM (top), HF/RSA (middle), and SDNN (bottom). The plots show one data point per participant (19 total) resulting from HRV analysis of each corresponding 5-minute, IXI time series.

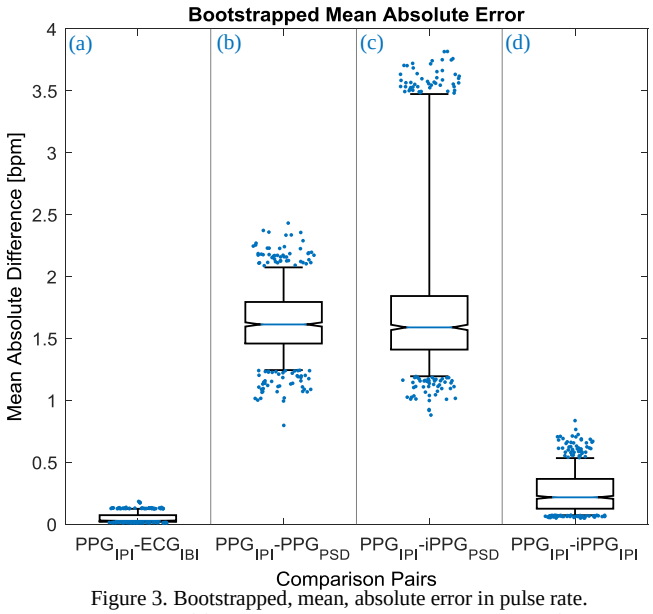

Figure 3. Bootstrapped, mean, absolute error in pulse rate. Comparisons of fingertip PPG with individual BVP identification versus: (a) ECG using IBIs, (b) contact PPG using periodograms, (c) long-range iPPG using periodograms, and (d) long-range iPPG using IPIs. Error means were randomly bootstrapped over 1000 iterations. Boxes represent the first, median, and third quartiles. Whiskers represent the 95% CI for each bootstrapped distribution, with the outlying 2.5% of points on either side plotted individually.

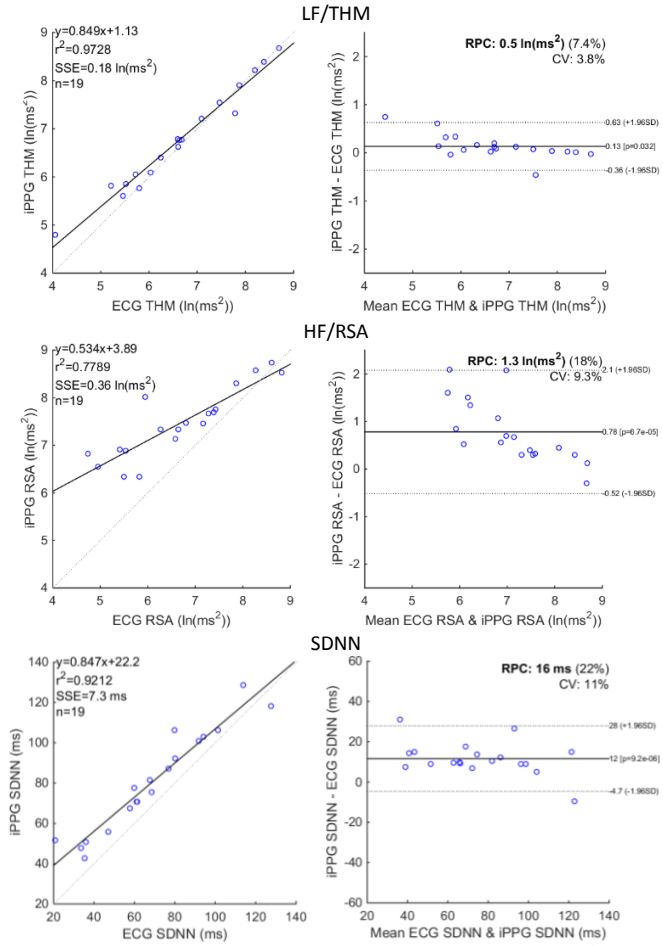

Figure 4. Side-by-side correlation and Bland-Altman plots for measurement comparison between PRV from long-range iPPG and HRV from gold-standard ECG. From top to bottom, LF/THM, HF/RSA, and SDNN variability measurements are compared.

IV. Discussion

In this study we completed a further investigation into the capabilities of long-range imaging photoplethysmography by employing a high-quality digital camera and super-telephoto lens. Previous studies have typically occupied the range of imager-to-subject distances of a few centimeters to a maximum of 3 meters. Our recently published work [21] demonstrated measurements of pulse rate at distances of 25, 50, and 100 meters by employing the periodogram approach. For that method, mean absolute error increased with distance as signal quality diminished, likely due to the decreased facial region size in the image as well as the greatly diminished light transmitted to the image sensor with increased focal lengths. A relative strength of the periodogram approach was shown in its ability to recover pulse rates within 2.0, 4.1, and 10.9 beats per minute of mean absolute error at imager-to-subject distances of 25, 50, and 100 meters, respectively, over a pool of 22 subjects. This was possible even when component waveforms were very noisy and BVP waves were indistinguishable in the time series data, as was especially true at distances of 50 and 100 meters [21]. However, a weakness of the periodogram approach was demonstrated by an estimated 1.34 beats per minute of mean absolute error contributed by the periodogram method. This weakness is attributable to the oversimplification of estimating an individual's time-varying pulse rate using a single dominate frequency within a given windowed signal where other noise is present. In this work using iPPG waveforms recovered at 25 meters, individual BVP waves were identified and used to significantly improve the accuracy of the windowed pulse rate estimates as well as enable accurate measurements of pulse rate variability.

The various comparisons of pulse rate estimation methods, shown in Fig. 3, illustrate several important points regarding the possible choices for heart/pulse rate measurement. As shown in the Fig. 3(a), pulse rate derived from contact, fingertip PPG and heart rate derived from ECG, each with individual cardiac cycle identification, are essentially equivalent for individuals at rest with every bootstrap point falling below 0.18 bpm of mean absolute difference. This correspondence is expected based on a review of the published literature [25]. Consequently, subsequent comparisons are made with respect to the fingertip PPG data with individual cycle identification. Fig. 3(b) shows the methodological error resulting from the periodogram method by comparing pulse rate estimation method (individual cycle identification vs periodogram) for fingertip PPG. From this comparison, approximately 1.6 bpm of mean absolute error and considerable additional variability is attributed to the periodogram method. Fig. 3(c) shows the absolute error distributions for pulse rates derived using the periodogram method for long-range iPPG with a mean error of the bootstrap distribution of 1.59 bpm. As recently published [21], much of this difference was attributed to the methodological error resulting from the periodogram approach, by analogy to the comparison shown in Fig. 3(b) for contact PPG. After completing individual cycle identification in this study, Fig. 3(d) confirms that assertion and demonstrates a significant decrease in absolute error and thus increase in accuracy. The mean absolute error for the bootstrap distribution was 0.22 bpm with all individual

bootstrap data points falling below 0.83 bpm. This demonstrates that very accurate measurements of windowed pulse rate can be achieved at long imager-to-subject distances up to 25 meters for stationary subjects.

The correlation and Bland-Altman plots presented in Fig. 4 show high correlations and good limits of agreement for the comparisons of heart rate variability measures from long-range iPPG vs gold-standard ECG. While positive mean offsets/ biases are observed, each of the HRV measures are well correlated. This general overestimation of short-term variability is expected and has been observed in several studies of contact PPG [25]. These results agree well with other published estimates of heart rate variability using iPPG at imager-to-subject distances up to 3m [30]-[35] and show promise that iPPG may be used to assess meaningful health or stress states as shown in [31], even at long imager-to-subject distances.

As demonstrated in this study, the significant improvement in pulse rate measurement accuracy and the ability to recover highly correlated (to ECG-derived, gold standard) measurements of PRV, even at exceedingly long imager-to-subject distances, is an exciting demonstration of the capabilities of iPPG. For stationary subjects, accuracy comparable to close range iPPG measurements of PR and PRV was achieved using a consumer, enthusiast grade digital camera and relatively inexpensive super-telephoto lens. Despite these successes, further exploration is required to better understand long-range iPPG. The recovered signals from three individuals were too noisy to be recovered and signals measured at distances greater than 25m did not contain consistently identifiable BVP waves and were excluded from analysis. Additionally, effects of subject motion on long-range iPPG were not studied but would likely pose significant challenges for signal recovery, similar to close-range iPPG.

Future studies may evaluate long-range iPPG outdoors in daylight conditions when measured illuminance ranges from 10,000 to 25,000 lux, providing 10-25x better subject illumination than provided by the artificial lighting used in this study [44]. Additionally, the use of multiple imagers recording video simultaneously [45], [46], color space based methods [47], and/or targeted facial regions of interest [48] may be used to aid in iPPG signal recovery. More generally, the effects of other variables of interest which may affect iPPG signal quality including participant characteristics (skin tone, age, gender, facial hair, skincare product/ makeup use) and varying lighting and image background conditions may be examined in larger sample sizes and/or by explicitly controlling for these factors of interest. Finally, multi-spectral evaluation of iPPG may be used to examine potential advantages resulting from utilizing spectral bands other than red, green, and, blue as recently demonstrated using a five-band (red, green, blue, cyan, and orange) imager [30].

V. Conclusion

This study demonstrated the first measurement of pulse rate variability using long-range imaging photoplethysmography and also demonstrated improved pulse rate measurement accuracy. At a distance of 25 meters, iPPG waveforms were recovered with very good correlation to fingertip PPG and ECG for 19 participants seated at rest. This enabled the accurate identification of individual blood volume pulse waves and measurements of pulse rate variability (LF/THM, HF/RSA, SDNN) and windowed pulse rate compared to gold-standard ECG. Using individual cardiac cycle identification, as compared to the periodogram approach to measure pulse rate, reduced the mean absolute error in the estimate from 1.6 to 0.2 beats per minute. Correlation analysis (r^2) between the camera-based measures of pulse rate variability and ECG-derived heart rate variability ranged from 0.779 to 0.973. These results are comparable to those accuracies previously demonstrated with imager-to-subject distances of no more than 3 meters. This study demonstrates that pulse rates within one beat-per-minute of that obtained by gold-standard ECG can be achieved when the recovered blood volume pulse morphology is of adequate quality to resolve systolic onsets for individual cardiac cycles. Further, this same approach can yield data of very promising quality for estimating measures of pulse rate variability.

References

[1] L. A. M. Aarts, V. Jeanne, J. P. Cleary, C. Lieber, J. S. Nelson, S. Bambang Oetomo and W. Verkruysse. Non-contact heart rate monitoring utilizing camera photoplethysmography in the neonatal intensive care unit: A pilot study. *Early Hum. Dev.* 89(12). pp. 943-948. 2013. DOI: 10.1016/j.earlhumdev.2013.09.016.

[2] J. H. Klaessens, M. van den Born, A. van der Veen, J. Sikkens-van de Kraats, F. A. van den Dungen and R. M. Verdaasdonk. Development of a baby friendly non-contact method for measuring vital signs: First results of clinical measurements in an open incubator at a neonatal intensive care unit. *Advanced Biomedical and Clinical Diagnostic Systems XII* 2014. DOI: 10.1117/12.2038353.

[3] M. Villarroel, S. Davis, P. Watkinson, A. Guazzi, K. McCormick, L. Tarassenko, J. Jorge, A. Shenvi and G. Green. Continuous non-contact vital sign monitoring in neonatal intensive care unit. *Healthcare Technology Letters 1(3),* pp. 87-91. 2014. DOI:10.1049/htl.2014.0077.

[4] D. Shao, Y. Yang, C. Liu, F. Tsow, H. Yu and N. Tao. Noncontact monitoring breathing pattern, exhalation flow rate and pulse transit time. *IEEE Trans. Biomed. Eng. 61(11),* pp. 2760-2767. 2014. DOI: 10.1109/tbme.2014.2327024.

[5] N. Blanik, A. K. Abbas, B. Venema, V. Blazek and S. Leonhardt. Hybrid optical imaging technology for long-term remote monitoring of skin perfusion and temperature behavior. *J. Biomed. Opt. 19(1),* pp. 016012. 2014. DOI: 10.1117/1.jbo.19.1.016012.

[6] U. Rubins, V. Upmalis, O. Rubenis, D. Jakovels and J. Spigulis. Real-time photoplethysmography imaging system. *IFMBE Proceedings, 15th Nordic-Baltic Conference (NBC) on Biomedical Engineering and Medical Physics* pp. 183-186. 2011. DOI: 10.1007/978-3-642-21683-1_46.

[7] W. Mo, R. Mohan, W. Li, X. Zhang, E. W. Sellke, W. Fan, J. M. DiMaio and J. E. Thatcher. The importance of illumination in a non-contact photoplethysmography imaging system for burn wound assessment. *Proc. SPIE, Photonic Therapeutics and Diagnostics XI* 2015. DOI: 10.1117/12.2080699.

[8] R. Imms, S. Hu, V. Azorin-Peris, M. Trico and R. Summers. A high performance biometric signal and image processing method to reveal blood perfusion towards 3D oxygen saturation mapping. *Proc. SPIE, Imaging, Manipulation, and Analysis of Biomolecules, Cells, and Tissues XII* 2014. DOI: 10.1117/12.2044318.

[9] L. Kong, Y. Zhao, L. Dong, Y. Jian, X. Jin, B. Li, Y. Feng, M. Liu, X. Liu and H. Wu. Non-contact detection of oxygen saturation based on visible light imaging device using ambient light. *Opt. Express 21(15),* pp. 17464. 2013. DOI: 10.1364/oe.21.017464.

[10] Y. Sun and N. Thakor. Photoplethysmography revisited: From contact to noncontact, from point to imaging. *IEEE Trans. Biomed. Eng. 63(3),* pp. 463-477. 2016. DOI: 10.1109/tbme.2015.2476337

[11] D. J. McDuff, J. R. Estepp, A. M. Piasecki and E. B. Blackford. A survey of remote optical photoplethysmographic imaging methods. *37th Annu. Int. Conf. IEEE Engineering in Medicine and Biology Society (EMBC)* pp. 6398-6404. 2015. DOI: 10.1109/embc.2015.7319857.

[12] Kranjec, J., Beguš, S., Geršak, G. and Drnovšek, J., "Non-contact heart rate and heart rate variability measurements: A review," J. Biomed. Sig. Proc. and Control 13(0), pp. 102-112. 2014.

[13] J. Allen and K. Howell. Microvascular imaging: Techniques and opportunities for clinical physiological measurements. *Physiol. Meas. 35(7)*, pp. 91-141. 2014. DOI: 10.1088/0967-3334/35/7/r91.

[14] D. Teichmann, C. Bruser, B. Eilebrecht, A. Abbas, N. Blanik and S. Leonhardt. Non-contact monitoring techniques - principles and applications. *Annu. Int. Conf. IEEE Engineering in Medicine and Biology Society (EMBC)* pp. 1302-1305. 2012. DOI: 10.1109/embc.2012.6346176.

[15] He Liu, Yadong Wang and Lei Wang. A review of non-contact, low-cost physiological information measurement based on photoplethysmographic imaging. *Annu. Int. Conf. IEEE Engineering in Medicine and Biology Society(EMBC)* pp. 2088-2091. 2012. DOI: 10.1109/embc.2012.6346371.

[16] Sijung Hu, V. A. Peris, A. Echiadis, Jia Zheng and Ping Shi. Development of effective photoplethysmographic measurement techniques: From contact to non-contact and from point to imaging. *Annu. Int. Conf. IEEE Engineering in Medicine and Biology Society (EMBC)* pp. 6550-6553. 2009. DOI: 10.1109/iembs.2009.5334505.

[17] K. Charlot, J. Cornolo, J. V. Brugniaux, J. P. Richalet and A. Pichon. Interchangeability between heart rate and photoplethysmography variabilities during sympathetic stimulations. *Physiol. Meas. 30(12)*, pp. 1357-1369. 2009. DOI: 10.1088/0967-3334/30/12/005.

[18] E. Gil, M. Orini, R. Bailón, J. Vergara, L. Mainardi and P. Laguna, "Photoplethysmography pulse rate variability as a surrogate measurement of heart rate variability during non-stationary conditions", *Physiol. Meas.*, vol. 31, no. 9, pp. 1271-1290, 2010.

[19] M. Malik, J. T. Bigger, A. J. Camm, R. E. Kleiger, A. Malliani, A. J. Moss and P. J. Schwartz. Heart rate variability: Standards of measurement, physiological interpretation, and clinical use. *Eur. Heart J. 17(3)*, pp. 354-381. 1996. DOI: 10.1093/oxfordjournals.eurheartj.a014868.

[20] J. Allen. Photoplethysmography and its application in clinical physiological measurement. *Physiol. Meas. 28(3)*, pp. 1-39. 2007. DOI: 10.1088/0967-3334/28/3/r01.

[21] E. B. Blackford, J. R. Estepp, A. M. Piasecki, M. A. Bowers and S. L. Klosterman. Long-range non-contact imaging photoplethysmography: Cardiac pulse wave sensing at a distance. *Proc. SPIE, Optical Diagnostics and Sensing XVI: Toward Point-of-Care Diagnostics* 2016. DOI: 10.1117/12.2208130.

[22] C. Chuang, J. Ye, W. Lin, K. Lee and Y. Tai. Photoplethysmography variability as an alternative approach to obtain heart rate variability information in chronic pain patient. *J. Clin. Monit. Comput. 29(6)*, pp. 801-806. 2015. DOI: 10.1007/s10877-015-9669-8.

[23] X. Chen, Y. Huang, F. Yun, T. Chen and J. Li. Effect of changes in sympathovagal balance on the accuracy of heart rate variability obtained from photoplethysmography. *Experimental and Therapeutic Medicine* 2015. . DOI: 10.3892/etm.2015.2784.

[24] H. Posada-Quintero, D. Delisle-Rodríguez, M. Cuadra-Sanz and R. Fernández de la Vara-Prieto, "Evaluation of pulse rate variability obtained by the pulse onsets of the photoplethysmographic signal", *Physiol. Meas.*, vol. 34, no. 2, pp. 179-187, 2013.

[25] A. Schäfer and J. Vagedes, "How accurate is pulse rate variability as an estimate of heart rate variability?". *Int. J. of Card.*, vol. 166, no. 1, pp. 15-29, 2013.

[26] D. Jarrin, J. McGrath, S. Giovanniello, P. Poirier and M. Lambert, "Measurement fidelity of heart rate variability signal processing: The devil is in the details", *Int. J. of Psych.*, vol. 86, no. 1, pp. 88-97, 2012.

[27] P. Shi, Y. Zhu, J. Allen and S. Hu, "Analysis of pulse rate variability derived from photoplethysmography with the combination of lagged Poincaré plots and spectral characteristics", *Medical Engineering & Physics*, vol. 31, no. 7, pp. 866-871, 2009.

[28] P. Shi, S. Hu and Zhu, "A preliminary attempt to understand compatibility of photoplethysmographic pulse rate variability with electrocardiogramic heart rate variability", *J. Med. Biol. Eng.*, vol. 28, no. 4, pp. 173-180, 2008.

[29] N. D. Giardino, P. M. Lehrer and R. Edelberg. Comparison of finger plethysmograph to ECG in the measurement of heart rate variability. *Psychophysiology 39(2)*, pp. 246-253. 2002. DOI: 10.1111/1469-8986.3920246.

[30] D. McDuff, S. Gontarek and R. Picard, "Improvements in Remote Cardiopulmonary Measurement Using a Five Band Digital Camera", *IEEE Trans. Biomed. Eng.*, vol. 61, no. 10, pp. 2593-2601, 2014.

[31] D. McDuff, S. Gontarek and R. Picard. Remote measurement of cognitive stress via heart rate variability. *2014 36th Annu. Int. Conf. IEEE Engineering in Medicine and Biology Society (EMBC)* pp. 2957-2960. 2014. DOI: 10.1109/embc.2014.6944243.

[32] Y. Sun, S. Hu, V. Azorin-Peris, R. Kalawsky and S. Greenwald, "Noncontact imaging photoplethysmography to effectively access pulse rate variability", *J. Biomed. Opt*, vol. 18, no. 6, p. 061205, 2012.

[33] M. Poh, D. McDuff and R. Picard, "Advancements in Noncontact, Multiparameter Physiological Measurements Using a Webcam", *IEEE Trans. Biomed. Eng.*, vol. 58, no. 1, pp. 7-11, 2011.

[34] P. Shi, V. Peris, A. Echiadis, J. Zheng, Y. Zhu, P. Cheang and S. Hu, "Non-contact Reflection Photoplethysmography Towards Effective Human Physiological Monitoring", *J. Med. Biol. Eng*, vol. 30, no. 3, pp. 161-167, 2016.

[35] P. Shi, S. Hu, A. Echiadis, V. Azorin Peris, J. Zheng and Y. Zhu, "Development of a remote photoplethysmographic technique for human biometrics", *Proc. SPIE 7170, Design and Quality for Biomedical Technologies II*, p. 717006, 2009.

[36] J. Pan and W. J. Tompkins. A real-time QRS detection algorithm. *IEEE Trans. Biomed. Eng. BME-32(3)*, pp. 230-236. 1985. DOI: 10.1109/tbme.1985.325532.

[37] P. S. Hamilton and W. J. Tompkins. Quantitative investigation of QRS detection rules using the MIT/BIH arrhythmia database. *IEEE Trans. Biomed. Eng. BME-33(12)*, pp. 1157-1165. 1986. DOI: 10.1109/tbme.1986.325695.

[38] N. Yoder, "Peakfinder", *Mathworks File Exchange*, 2009. http://www.mathworks.com/matlabcentral/fileexchange/25500-peakfinder. [Accessed: 16- Jan- 2013].

[39] CardioBatch software. Brain-Body Center, University of Illinois at Chicago. 2007.

[40] S. Porges, "Method and Apparatus for Evaluating Rhythmic Oscillations in Aperiodic Physiological Response Systems", United States Patent 4,510,944, 1985.

[41] S. Porges and R. Bohrer, "Analyses of periodic processes in psychophysiological research", in *Principles of psychophysiology: Physical, social, and inferential elements*, 1st ed., J. Cacioppo and L. Tassinary, Ed. Cambridge University Press, 1990.

[42] R. Klein, "Bland-Altman and Correlation Plot", *Mathworks File Exchange*, 2014. http://www.mathworks.com/matlabcentral/fileexchange/45049-bland-altman-and-correlation-plot. [Accessed: 02- Feb- 2016].

[43] J. Martin Bland and D. Altman, "Statistical Methods for Assessing Agreement Between Two Methods of Clinical Measurement", *The Lancet*, vol. 327, no. 8476, pp. 307-310, 1986.

[44] P. Schlyter. Radiometry and photometry in astronomy. http://stjarnhimlen.se/comp/radfaq.html. [Accessed: 02- Feb- 2016].

[45] J. R. Estepp, E. B. Blackford and C. M. Meier. Recovering pulse rate during motion artifact with a multi-imager array for non-contact imaging photoplethysmography. *2014 IEEE Int. Conf. on Systems, Man, and Cybernetics (SMC)* pp. 14262-14269. 2014. DOI: 10.1109/smc.2014.6974121.

[46] E. B. Blackford and J. R. Estepp. Effects of frame rate and image resolution on pulse rate measured using multiple camera imaging photoplethysmography. *Proc. SPIE, Medical Imaging: Biomedical Applications in Molecular, Structural, and Functional Imaging* pp. 94172D, 1-14. 2015. DOI: 10.1117/12.2083940.

[47] G. de Haan and A. Van Leest. Improved motion robustness of remote-PPG by using the blood volume pulse signature. *J. Phys. Meas. 35(9)*, pp. 1913-1926. 2014. DOI: 10.1088/0967-3334/35/9/1913.

[48] H. E. Tasli, A. Gudi and M. den Uyl. Remote PPG based vital sign measurement using adaptive facial regions. *2014 IEEE Int. Conf. on Image Processing (ICIP)* pp. 1410-1414. 2014. DOI: 10.1109/icip.2014.7025282.